

LRP 672/00

August 2000

**Plastic Flow Localization
in Irradiated Materials:
A Multiscale Modeling Approach**

T. Diaz de la Rubia, H.M. Zbib, T.A. Kraishi,
B.D. Wirth, M. Victoria and M.-J. Caturla

Accepted for publication in NATURE

ISSN 0458-5895

Plastic Flow Localization in Irradiated Materials: A Multiscale Modeling Approach

T. Diaz de la Rubia¹, H.M. Zbib², T.A. Kraishi², B.D. Wirth¹, M. Victoria³ and M.-J. Caturla¹

- 1) Lawrence Livermore National Laboratory, Livermore, CA, USA.
- 2) Washington State University, Pullman, WA, USA.
- 3) EPFL-CRPP Fusion Technology Materials, Villigen PSI, Switzerland.

Accepted for publication in Nature

February, 2000

Plastic flow localization in irradiated materials: a multiscale modeling approach

Tomas Diaz de la Rubia^{*}, Hussein M. Zbib[†], Tariq A. Khraishi[†], Brian D. Wirth^{*},

Max Victoria[‡], & Maria Jose Caturla^{*}

^{*} *Lawrence Livermore National Laboratory, Livermore, California 94550, USA,*

[†] *Washington State University, Pullman, Washington 99164, USA,*

[‡] *EPFL-CRPP-Fusion Technology Materials, 5232 Villigen PSI, Switzerland*

When deformed after irradiation with energetic particles, metals exhibit increased yield stress and often undergo plastic flow localization and significant degradation of their mechanical properties^{1,2}. The effect limits the lifetime of the pressure vessel in most of the world's nuclear power plants³, and threatens to severely limit the choice of materials for the development of fusion-based alternative energy sources⁴. While these phenomena have been known for many years¹, an explanation of the underlying fundamental mechanisms and their relation to the irradiation field is lacking. Here, we use a multiscale simulation to show that the localization of plastic flow in defect-free channels results from a combination of dislocation pinning by irradiation-induced defect clusters, unpinning by defect unfauling and absorption, and cross slip of the dislocation as the stress is increased. Double cross slip induces dipole formation and this limits the channel width. The ensuing plastic instability results in catastrophic mechanical failure.

The microstructure of irradiated materials evolves over a wide range of length and time scales, making radiation damage an inherently multiscale phenomenon. At the shortest scales (nm and picoseconds), recoil-induced cascades of energetic atomic displacements give rise to a highly non-equilibrium concentration of point defects and point defect clusters⁵. Over macroscopic length and time scales these defects can migrate and alter the chemistry and microstructure, often inducing significant degradation of mechanical and other properties^{1,2}. In metals, the key features of neutron or ion beam irradiation-induced mechanical behavior can be summarized as²: (a) a sharp increase in yield stress with irradiation dose, (b) the appearance of a yield point followed by a yield drop in FCC metals, and perhaps most interestingly, (c) an instability that results in plastic flow localization within so-called “dislocation channels” and leads to loss of ductility and premature failure. An example of flow localization is shown in Fig. 1⁶. The Transmission Electron Microscopy (TEM) image shows a channel where all visible irradiation-induced point defect clusters are absent and where uniform large shear (about 100%) has taken place. The channels are 100 to 200 nm wide. Plastic flow localization is responsible for the observed loss of ductility.

Early theories of irradiation hardening focused on various source and dispersed barrier mechanisms^{7,8}. More recently, Trinkaus et al^{9,10} have proposed the analytical Cascade-Induced Source Hardening (CISH) model. This model uses insights from molecular dynamics (MD) simulations¹¹⁻¹⁴ and accounts for some of the recent experimental observations. In the model, it is postulated that interstitial clusters produced in displacement cascades form glissile dislocation loops that migrate in one dimension by thermally activated glide and decorate dislocations, thereby pinning them. However, while this model provides a rational explanation for the observed increase in yield stress, it does not explain plastic flow localization and the development of plastic instabilities.

In the following, we couple these experimental and atomistic simulation results¹¹⁻¹⁸ to a three-dimensional dislocation dynamics (DD) simulation to investigate the relation between the irradiation field and mechanical behavior. We consider two cases, Cu and Pd, which exhibit different damage morphologies under irradiation. Experiments have shown that vacancy stacking-fault tetrahedra (SFTs) are the predominant defect type in low stacking fault energy Cu^{6,19}, whereas in high stacking fault energy Pd, self-interstitial atom Frank-sessile (FS) loops constitute the majority of observed defects^{20,21}. Our DD simulation box is a cube 5 μm in size that contains an initial density of Frank-Read (FR) dislocation sources distributed at random on $\{111\}$ planes. In our DD simulation²²⁻²⁴, the plastic deformation of a single crystal is obtained by explicit accounting of the dislocation evolution history, i.e. their motion and structure.

The motion and interaction of an ensemble of dislocations in a three-dimensional crystal is marched in time. Dislocations are discretized into straight-line segments of mixed character. The Peach-Koehler force F acting on a dislocation segment inside the computational cell is calculated from the stress fields due to immediate neighboring segments, all other dislocations segments, all defect clusters, and the applied stress. The result is used to advance the dislocation segment based on a linear mobility model, $v_{gi} = M_{gi} F_{gi}$, where v_{gi} is the glide velocity of the dislocation segment, M_{gi} is the dislocation mobility, and F_{gi} is the glide component of the Peach-Koehler force minus the Peierl's friction. Based on the history of dislocation motion, one obtains a measure for the macroscopic plastic strain rate. To ensure continuity of dislocation lines across the boundaries, we apply reflection boundary conditions as described by Zbib et al²². Due to the long-range character of the dislocation stress field, long-range interactions are computed explicitly²².

In the simulation, segments that are on the verge of experiencing short-range interactions are identified. Based on a set of physical rules, such reactions may result in the formation of junctions, jogs, dipoles, etc. The dislocations multiply by a variety of mechanisms that may involve superjog collisions²⁵, standard Frank-Read source multiplication, and double cross slip. Cross slip is described as an activated process with probability, P , given by

$$P = \alpha \Omega_1 \delta t \exp\left(-\frac{\Delta W^* - \tau A}{kT}\right), \quad \Omega_1 = \frac{C_t \pi}{L}$$

where Ω_1 is the fundamental frequency of a vibrating dislocation segment of length L , C_t is the transverse sound velocity, δt is the time increment, α is a numerical parameter controlling the frequency of cross slip, ΔW^* is the activation energy for cross-slip²³, τ is the resolved shear stress, A is the area swept by the dislocation segment that undergoes cross-slip and kT has its usual meaning.

The irradiation field is modeled by mapping into the DD box the spatial distribution of defect clusters (SFTs and/or FS interstitial loops) that results from a particular irradiation fluence, temperature and particle energy. At room temperature, typical defect cluster radii are 0.5 to 3 nanometers and their density in the bulk, ρ_B , ranges from 10^{21} - 10^{24} m⁻³ depending on irradiation fluence^{17,19,20}. In the simulation, this translated into 100,000 to 2 million defect clusters. Following the CISH model^{9,10}, Frank-Read sources *decorated* along the dislocation line with defect clusters are also introduced into the DD simulation as described below.

Dislocation segments interact with the irradiation-induced defect clusters. The elastic interaction of a moving dislocation with a defect cluster (SFT or loop) can be obtained from elasticity theory. However, elasticity calculations cannot by themselves determine the fate of the defect cluster as it interacts with the moving dislocation. To address this point, we have performed MD simulations of dislocation-SFT interaction.

Figure 2 shows the results of a simulation involving 933,000 atoms at 100 K in Cu. In this simulation, overlapping truncated SFTs*, such as formed by aging displacement cascades¹⁷, with a spacing of 8.5 nm (along the dislocation line direction $\langle 112 \rangle$) are placed on the glide plane of a dissociated edge dislocation. The two partial dislocations then move under an applied shear stress of 300 MPa. Figure 2a shows that upon contact, the leading partial is initially pinned by the overlapping SFT. At a later time, Fig. 2b, the leading partial dislocation absorbs part of the overlapping SFT and climbs (clearly seen in $\langle 110 \rangle$ projection) as the trailing partial approaches. Finally, in Fig. 2c, we show that the trailing partial catches the leading partial at the location of the overlapping SFT, constricts and climbs by absorbing the remaining defect. Following absorption of the SFT, the dislocation continues to move but with reduced mobility as a result of the jogs that form on the constricted line segment. While this simulation clearly shows defect absorption, the case is not unique and we are currently investigating the matrix of possible interactions.

For Frank sessile dislocation loops (relevant to Pd), the elastic interaction is computed explicitly as described in Khraishi et al²⁶. Here the FS loop is absorbed by the dislocation line if the loop *unfaults* and becomes glissile. Following Ghoniem et al²⁷, one can calculate the energy difference, ΔE , between the faulted loop state and the unfaulted state (i.e. perfect loop), taking into account the interaction energy between the dislocation and the sweeping Shockley partials. When $\Delta E > 0$, the critical radius for loop unfaulting decreases and the loop may transform from the faulted sessile to the unfaulted glissile configuration. When the critical radius for unfaulting is reached, the loop gets absorbed at the core of the dislocation and the dislocation is able to move. Recently, Rodney and

*A triangular vacancy platelet that is bounded by $\langle 110 \rangle$ directions forms a single SFT. A triangular vacancy platelet bounded by two $\langle 110 \rangle$ and one $\langle 112 \rangle$ directions forms two partial SFTs, one above and one below the initial plane; we define this as an overlapping truncated SFT.

Martin²⁸ have carried out atomistic simulations for interstitial loops consistent with this model.

Fig. 3 shows the stress-strain curves obtained with our DD simulations for Cu irradiated to $\rho_B = 8.24 \times 10^{21} \text{ m}^{-3}$, which considering a uniform defect distribution corresponds to a SFT spacing of 50 nm. The initial network dislocation density is $\rho_N = 10^{12} \text{ m}^{-2}$. Without irradiation the system yields at about 37 MPa, and work hardening starts at the early stage of deformation as a result of dislocation multiplication and forest interactions. When irradiation-induced defects are present, two behaviors are seen. When the defect density along the line (ρ_D) is such that the average spacing is only 10 nm, i.e. $\rho_D \gg \rho_B$, a clear yield point followed by a yield drop can be observed. However, when the average spacing between defects along the dislocation line is 30 nm, which is comparable to that in the bulk, the system yields at a slightly higher stress and only a very diffuse yield drop is apparent. This is in excellent agreement with experiments⁵ which show that the observed yield drop disappears at elevated doses where $\rho_D \approx \rho_B$. The dose dependence of the yield stress obtained in our DD simulations of irradiated Pd (more details are given by Khraishi et al²⁹), where all the irradiation-induced defect clusters are Frank sessile dislocation loops, has a slope of 0.35, which is in excellent agreement with the experimental observations of Baluc et al²¹.

Figs. 4a and its projection into 2D Fig. 4b, show the results of our simulations in Cu where cross slip/double cross slip takes place and irradiation-induced SFT defects are absorbed by sweeping dislocations based on the criterion discussed above. The figures show localization of plastic flow in defect-free channels. The channel width is approximately 200 nm with a channel spacing of 1000 nm in agreement with experimental observations¹. Examination of the simulation results reveals that the mechanism of channel formation can be described as follows. As dislocations propagate

from a FR source a screw dislocation segment may be pinned by the defects and eventually cross slip from its primary plane as the stress is increased. This is followed by double cross slip of the segment, creating a new dislocation source on a parallel plane. This process continues with dislocations segments cross slipping progressively from one glide plane to another, resulting in a set of parallel planes with active dislocations (the spacing between each pair of planes varies between 25 to 50 nm). Eventually, spreading of the band is limited by the interaction between segments of opposite sign that, in concert with the defects, exert a back stress on those segments attempting to cross slip. However, the process is continuous with dislocations being emitted from the same original single source, cross slipping to adjacent planes and so on, resulting in a large local shear strain (about 100%) in the band. The spacing between the channels is a stochastic variable determined by the spatial distribution of dislocation sources.

In summary, we have presented a multiscale computer simulation that provides a physical description of the underlying mechanisms that govern plastic flow localization and mechanical failure in irradiated metals. New MD simulations demonstrate the mechanism of absorption of SFTs by moving edge dislocations. Our DD simulation couples these atomistic simulations and experiments to a mesoscale description of mechanical behavior. The results show that flow localization results from a combination of dislocation pinning by irradiation-induced defect clusters, unpinning by unfauling and absorption of the defect clusters, and cross slip of the dislocation as the stress is increased. Double cross slip results in dipole formation, which in a natural way self-limits the width of the channels. The plastic instability results in catastrophic mechanical failure.

References

1. Eyre, B.L. and Barlett, A.F. An electron microscope study of neutron irradiation damage on α -iron. *Phil. Mag.* **12** 261-271 (1965).
2. Victoria, M., *et al.* The microstructure and associated tensile properties of irradiated fcc and bcc metals. *J. Nucl. Mater.* **276**, 114-122 (2000).
3. Odette, G. R. & Lucas, G. E. Recent progress in understanding reactor pressure vessel steel embrittlement. *Rad. Effects and Defects in Sol.* **144**, 189-231 (1998).
4. Bloom, E. E. The challenge of developing structural materials for fusion power systems. *J. Nucl. Mater.* **258-263**, 7-17 (1998).
5. Averback, R.S. and Diaz de la Rubia, T. Fundamental mechanisms of radiation damage. *Solid State Physics*. Ed. by F. Spaepen and H. Ehrenreich, (Academic Press, NY, 1998) Vol 51, pp
6. Dai, Y. & Victoria, M. Defect cluster structure and tensile properties of Cu single crystals irradiated with 600 MeV protons. *MRS Symp. Proc.* **439**, 319-324 (1997).
7. Friedel, J. *Dislocations* (Pergamon Press, Oxford, 1964).
8. Bement, A.L., Fundamental materials problems in nuclear reactors. *Proc. 2nd Int. Conf. On Strength of Metals and Alloys*. Vol. **II**, 693-728 (1970).

9. Trinkaus, H., Singh, B. N. & Foreman, A. J. E. Segregation of cascade induced interstitial loops at dislocations: possible effect on initiation of plastic deformation. *J. Nucl. Mater.* **251**, 172-187 (1997).
10. Singh, B. N., Foreman, A. J. E. & Trinkaus, H. Radiation hardening revisited: role of intracascade clustering. *J. Nucl. Mater.* **249**, 103-115 (1997).
11. Diaz de la Rubia, T. & Guinan, M. W. New mechanism of defect production in metals: A molecular-dynamics study of interstitial-dislocation-loop formation in high-energy displacement cascades. *Phys. Rev. Lett.* **66**, 2766- 2769 (1991).
12. Foreman, A. J. E., Phythian, W. J. & English, C. A. The molecular dynamics simulation of irradiation damage cascades in copper using a many-body potential. *Phil. Mag. A* **66**, 671- 695 (1992).
13. Wirth, B. D., Odette, G. R., Maroudas, D., Lucas, G. E., *J. Nucl. Mater.* **244**, 185 (1997).
14. Osetsky, Y. N., Bacon, D. J. & Serra, A. Thermally activated glide of small dislocation loops in metals *Phil. Mag. Lett.* **79**, 273-282 (1999).
15. Wirth, B. D., Bulatov, V. & Diaz de la Rubia, T. Atomistic simulation of stacking fault tetrahedra formation in Cu. *Proc. Int. Conf. on Fusion Reactor Materials ICFRM-9*, accepted for publication in *J. Nucl. Mater.* (2000).
16. Heinisch, H. L. Computer simulation of high energy displacement cascades. *Rad. Effects and Defects in Sol.* **113**, 53- 73 (1990).
17. Caturla, M. J., et al. Comparative study of radiation damage accumulation in Cu and Fe. *J. Nucl. Mater.* **276**, 13-21 (2000).

18. Soneda, N. & Diaz de la Rubia T. Defect production, annealing kinetics and damage evolution in alpha-Fe: an atomic-scale computer simulation. *Phil. Mag. A* **78**, 995-1019 (1998).
19. Singh, B. N. & Zinkle, S. J. Defect accumulation in pure fcc metals in the transient regime: a review. *J. Nucl. Mater.* **206**, 212-229 (1993).
20. Baluc, N., Dai, Y. & Victoria, M. Plasticity and microstructure of irradiated Pd. *MRS Symp. Proc.* **540**, 555-560 (1999).
21. Baluc, N., *et al.* Comparison of the microstructure and tensile behavior irradiated fcc and bcc metals. *MRS Symp. Proc.* **540**, 539-548 (1999).
22. Zbib, H. M., Rhee, M. & Hirth, J. P. On plastic deformation and the dynamics of 3D dislocations *Int. J. Mech. Sci.* **40**, 113-127 (1998).
23. Rhee, M., Zbib, H. M., Hirth, J. P., Huang, H. & Diaz de la Rubia, T. Models for long/short range interactions in 3D dislocation simulation. *Modeling Simul. Mater. Sci. Eng.* **6**, 467-492 (1998).
24. Zbib, H. M., Diaz de la Rubia T., Rhee, M. & Hirth, J. P. 3D dislocation dynamics: stress-strain behavior and hardening mechanisms in fcc and bcc metals. *J. Nucl. Mater.* **276**, 154-165 (2000).
25. Rhee, M., Lassila, D. H., Bulatov, V. V., Hshuing, L. & Diaz de la Rubia, T. Dislocation multiplication and the early stages of plastic deformation in bcc Molybdenum: a dislocation dynamics numerical simulation. *Phys. Rev. Lett.*, in review.

26. Khraishi, T. A., Zbib, H. M., Hirth, J. P. & Diaz de la Rubia, T. The stress field of a general circular Volterra dislocation loop: analytical and numerical approaches. *Phil. Mag. Lett.* **80**, 95-105 (2000).
27. Ghoniem, N. M., Singh, B. N., Sun., L. Z. & Diaz de la Rubia, T. Interaction and accumulation of glissile defect clusters near dislocations. *J. Nucl. Mater.* **276**, 166-177 (2000).
28. Rodney, D, and Martin, G, Dislocation pinning by small interstitial loops: a molecular dynamics study, *Phys. Rev. Lett.*, **82**, 3272-5 (1999)
29. Khraishi, T.A., Zbib, H.M., Diaz de la Rubia, T. & Victoria, M. Localized Deformation and Hardening in Irradiated Metals: 3D Discrete Dislocation Dynamics Simulations. *Acta Metall. Et Mater.*, submitted (2000).

Acknowledgements. This work was performed in part under the auspices of the U.S. Department of Energy by Lawrence Livermore National Laboratory. Work by M.V. was performed under a contract of the Swiss National Research Fund.

Figure Captions:

Figure 1. Defect-free channel in deformed irradiated Cu. Weak Beam Dark Field Transmission Electron Microscope image shows defect-free channels formed during deformation of Copper irradiated with 600 MeV protons⁵.

Figure 2. MD simulation of the interaction between an edge dislocation and a vacancy SFT in Cu. $\langle 111 \rangle$ (top) and $\langle 110 \rangle$ (bottom) projections of high energy atoms show the motion of two Shockley partials on their $\{111\}$ glide plane and their interaction with an overlapping vacancy SFT at a) 7.2 b) 16.0 and c) 16.8 ps after application of a 300 MPa shear stress.

Fig. 3. DD results of stress-strain curves. The stress-strain curves obtained with our DD simulations for Cu irradiated to $\rho_B = 8.24 \times 10^{21} \text{ m}^{-3}$. Without irradiation the systems yields at about 37 MPa. When the defect density along the line (ρ_D) is such that $\rho_D \gg \rho_B$, a clear yield point followed by a yield drop can be observed. However, when the average spacing between defects along the dislocation line is 30 nm, which is comparable to that in the bulk, the system yields at a slightly higher stress and only a very diffuse yield drop is apparent.

Fig. 4. DD results of channel formation and flow localization. a) results of DD simulation in Cu irradiated to $\rho_B = 8.24 \times 10^{21} \text{ m}^{-3}$ with initial network dislocation density of $\rho_N = 10^{12} \text{ m}^{-2}$, the figure shows the $10 \mu\text{m}$ side computational cell containing the dislocations and point defects with defect-free channels; b) 2D projection of Fig. 4a.

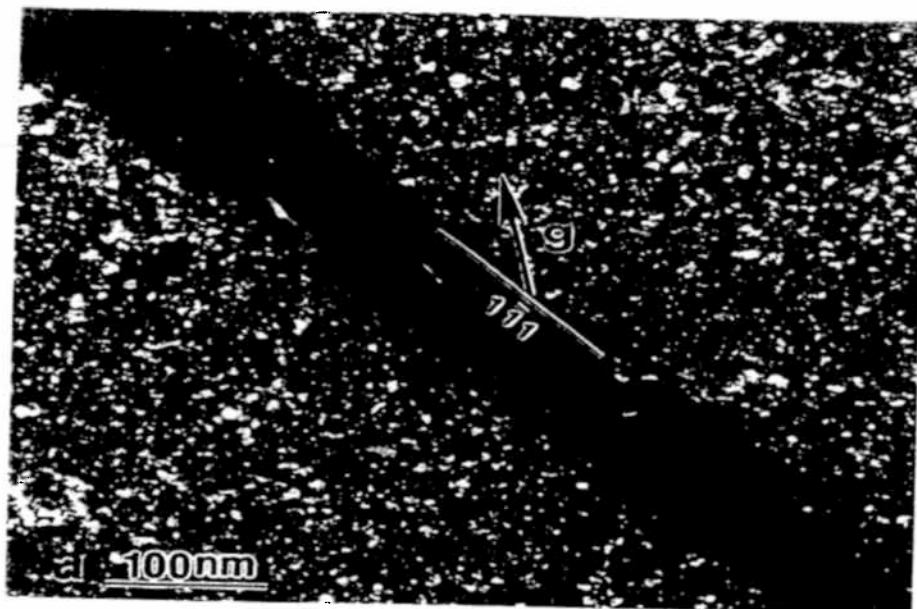


Figure 1.

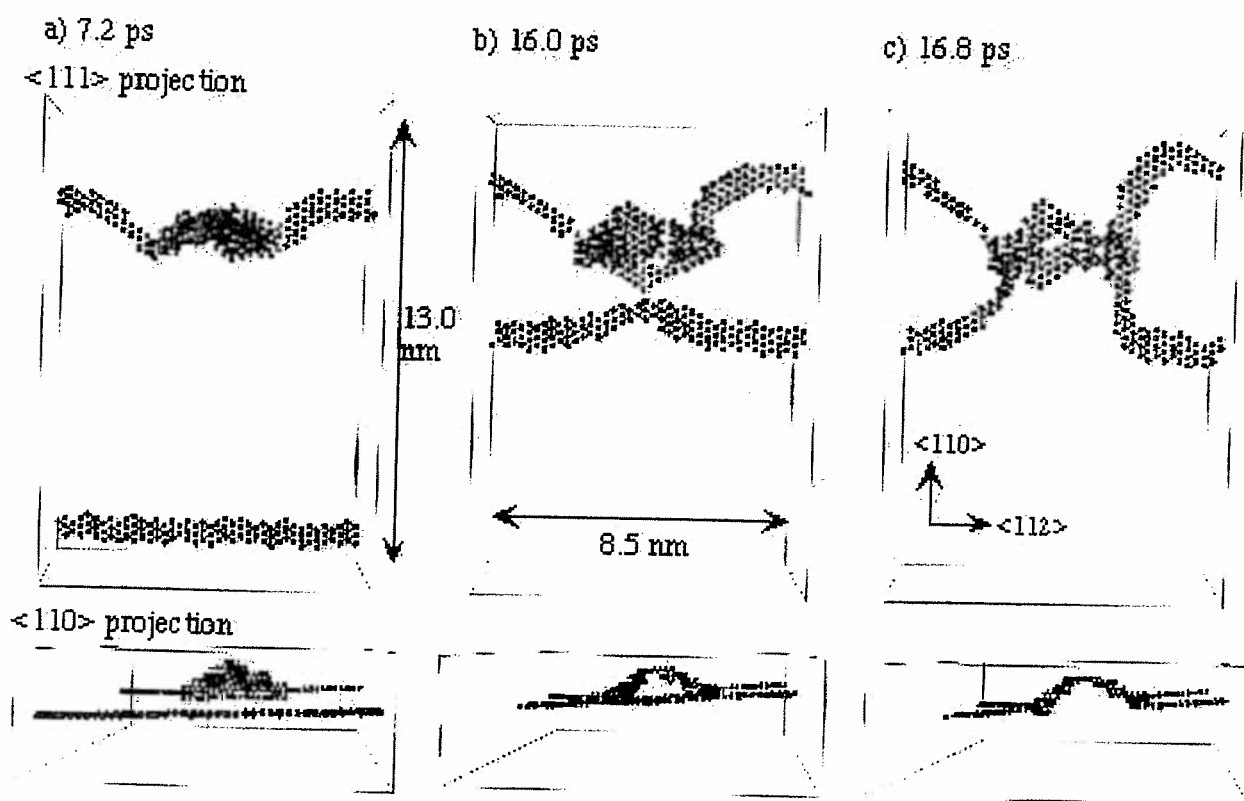


Figure 2 -- $\langle 111 \rangle$ (top) and $\langle 110 \rangle$ (bottom) projections of high energy atoms showing the motion of two Shockley partials on their $\{111\}$ glide plane and interaction with an overlapping SFT at a) 7.2, b) 16.0 and c) 16.8 ps after application of a shear stress.

Figure 2.

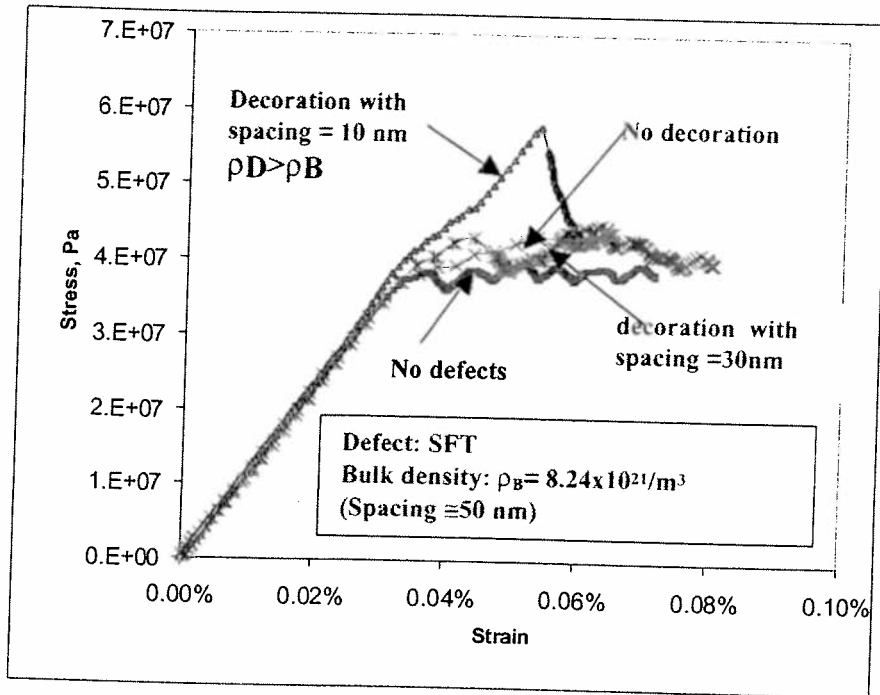


Figure 3

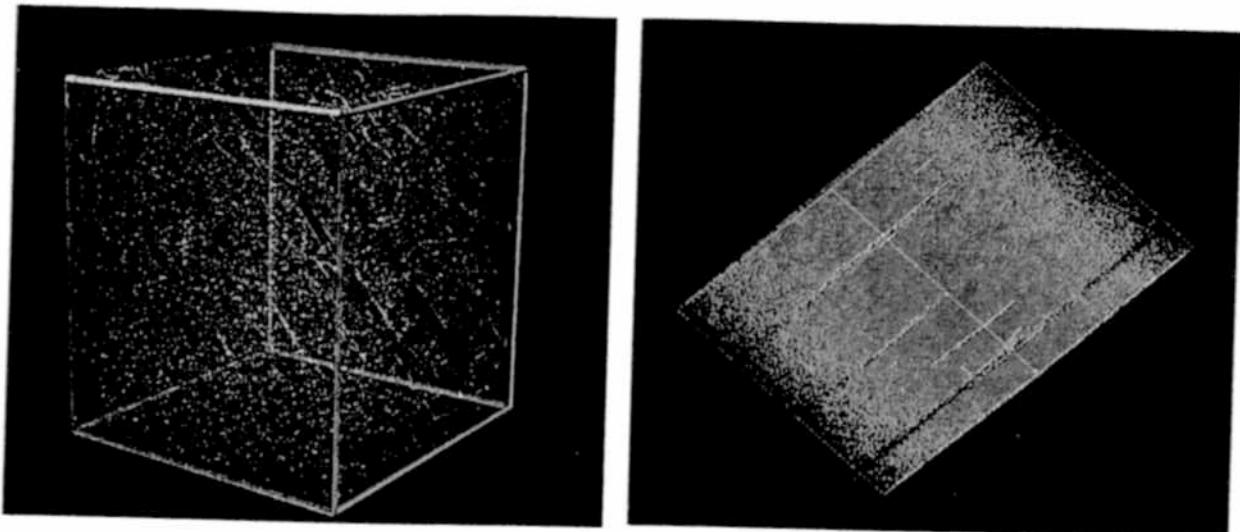


Figure 4 a),b)